OPEN ACCESS
International Journal of Neural Systems, Vol. 35, No. 13 (2025) 2550082 (14 pages)
© The Author(s)
DOI: 10.1142/S0129065725500820

World Scientific
www.worldscientific.com

Int. J. Neur. Syst. 2025.35. Downloaded from www.worldscientific.com
by KATHOLIEKE UNIVERSITEIT LEUVEN on 12/23/25. Re-use and distribution is strictly not permitted, except for Open Access articles.

# Subthalamic Nucleus Deep Brain Stimulation Modulates Auditory Steady State Responses in Parkinson's Disease

Thomas Pirenne
*Department of Neurosciences, Laboratory for Neuro- and Psychophysiology, KU Leuven, Leuven, Belgium*

Mansoureh Fahimi Hnazaee
*Wellcome Centre for Human Neuroimaging, Queen Square Institute of Neurology, University College London, London, UK*

Patrick Santens
*Department of Neurology, Ghent University Hospital, Ghent, Belgium*

Aline Moorkens and Marc M. Van Hulle*
*Department of Neurosciences, Laboratory for Neuro- and Psychophysiology, KU Leuven, Leuven, Belgium*
**marc.vanhulle@kuleuven.be*

Received 2 September 2025
Accepted 5 November 2025
Published Online 10 December 2025

Deficits in auditory perception have been widely observed in Parkinson's disease (PD) patients and the literature attributes it, in part, to impaired central auditory processing. Deep brain stimulation (DBS) of the subthalamic nucleus (STN) is a well-established therapeutic option for patients with advanced PD. Analysis of auditory evoked potentials suggested a modulatory effect of DBS on central auditory processing. To better understand the latter, we investigated whether DBS modulates auditory steady state responses (ASSR) in electroencephalography (EEG) recordings of 5 PD patients. ASSRs are neural responses along central auditory pathways phase-locked to an auditory stimulus which can serve to understand the spectral aspects of central auditory processing. In our analyses, we estimate the intensity of ASSRs with a novel method based on canonical correlation analysis (CCA) and compare them in DBS ON and OFF conditions. Our results suggest that DBS effectively reduces ASSR in patients with PD. A comparison to age-matched healthy participants suggests a pathological effect of PD on ASSRs, which is disrupted by DBS. These findings support our hypothesis that DBS suppresses central auditory processing. Further research is required to assess the symptomatic effect of this modulation, as well as which cortical and subcortical generators are most affected. A better understanding of the auditory side-effects of DBS could lead to improved treatment options.

*Corresponding author.

This is an Open Access article published by World Scientific Publishing Company. It is distributed under the terms of the Creative Commons Attribution 4.0 (CC BY) License, which permits use, distribution and reproduction in any medium, provided the original work is properly cited.

*Keywords*: Deep brain stimulation (DBS); Parkinson's disease; electroencephalography (EEG); auditory steady-state responses (ASSR); modulation; canonical correlation analysis (CCA).

Int. J. Neur. Syst. 2025.35. Downloaded from www.worldscientific.com
by KATHOLIEKE UNIVERSITEIT LEUVEN on 12/23/25. Re-use and distribution is strictly not permitted, except for Open Access articles.

## 1. Introduction

Parkinson's disease (PD) is a progressive nervous system disorder which, in its advanced stage, causes a considerable decrease in quality of life. Its progressive nature makes early detection of the disease a pivotal challenge for research to this day.[1,2] While the disease is mainly characterized by its motor symptoms, a better understanding of its nonmotor symptoms could help develop early biomarkers.[3] In well-defined patients, when pharmacological treatment fails to deliver relief, Deep Brain Stimulation (DBS) may provide an alternative treatment. Electrodes implanted in target nuclei of the basal ganglia such as the subthalamic nucleus (STN) are connected to a subcutaneous pulse generator that delivers electrical stimulation. Despite clinical success for over 30 years, the physiological mechanisms underlying Parkinsonism and the effects of DBS remain elusive.[4,5] While most studies have focused on the effects of DBS on the cardinal motor symptoms, nonmotor effects of DBS have been understudied.[6,7] Research was previously conducted to investigate whether motor-driven DBS has an effect on auditory processing.[8–10] Their results rely on auditory evoked potentials to establish that DBS modulates cortical auditory processing in patients with advanced PD.

It is increasingly accepted that impaired auditory processing is a potential nonmotor feature of PD.[11–13] In addition, auditory stimuli were shown capable of restoring PD brain activity to some extent, as well as affecting its motor symptoms.[14–16] Electrical stimulation was similarly proven capable of affecting phonation in PD.[17] Previous research investigating the effect of DBS on auditory processing focused on the cortex,[9,10] however, central auditory processing involves both cortical and deep sources ranging from the brainstem to the primary auditory cortex. Regarding deep sources, literature shows a clear involvement of the STN in auditory processing.[18,19] Therefore, it seems likely that auditory processing is affected by STN-DBS. Investigating the effect of DBS on the pathophysiology of PD requires high temporal resolution which can be obtained by electroencephalography (EEG) or magnetoencephalography (MEG) recordings. However, as DBS generates electrical artifacts which greatly hinder these recordings,[20,21] great care needs to be taken when analyzing such data.

In order to better understand the effect STN-DBS might have on central auditory processing, we investigated whether it modulates the amplitude of auditory steady state responses (ASSR). ASSRs are neural responses in the central auditory pathway i.e. mainly the auditory brainstem, the thalamus and the primary auditory cortex.[22] They are evoked in response to frequency-fixed auditory stimuli and known to reflect their temporal and spectral characteristics, rendering them suited to research central auditory processing. ASSRs are described by their amplitude and their phase. While the phase can provide a measure of latency between the different generators of the response along auditory pathways,[23] our focus is on whether the amplitude of the response is affected by DBS. We equipped 5 PD patients with EEG electrodes to record ASSRs in response to amplitude-modulated white noise auditory stimulation, modulated at different frequencies, when DBS is ON and OFF. We quantified ASSR intensities of DBS ON and OFF conditions and compared them statistically to investigate their modulation by DBS.

## 2. Materials and Methods

### 2.1. *DBS implantation*

Surgical procedures were performed by the DBS team of Ghent University Hospital in all recruited patients.[24] Electrode implantation was performed using a conventional stereotactic procedure with a combination of neuro-imaging guided anatomical targeting based on contrast-enhanced T1-weighted MRI, micro-electrode recording (Inomed, Emmendingen, Germany) and clinical evaluation of the effects of macro-electrode stimulation. The electrode location was verified post-operatively by comparing post- and pre-operative MRI scans. This confirmed the correct positioning of electrodes in the dorsolateral STN in all patients. A significant improvement

Int. J. Neur. Syst. 2025.35. Downloaded from www.worldscientific.com
by KATHOLIEKE UNIVERSITEIT LEUVEN on 12/23/25. Re-use and distribution is strictly not permitted, except for Open Access articles.

of motor symptoms was reported in all included patients during follow-up visits in the year after DBS surgery. Specifically, all patients reported an increase of at least 50% (range 50–100%) in DBS on-time without troublesome dyskinesia. Additionally, we noted clinical benefits of STN stimulation in all patients both intra-operatively and post-operatively in the short and long run. The participants are 5 PD patients whose anonymous stimulation details are shown in Table 1.

### 2.2. *Data collection*

Participants were tested in a room with a constant temperature of 20 degrees, sitting in front of an LCD screen at a distance of about 70 cm. During the experiment, a silent black and white movie was shown to prevent the participants from falling asleep. The stimuli consist of white noise with a bandwidth of 1 octave, centered at 1 kHz. They were 100% amplitude modulated at frequencies of 20, 40 and 80 Hz, and presented to both ears via ER-3A insert phones similarly to the work of Farahani *et al.*[26,22] to avoid microphonic and electromagnetic artifacts. Stimulus intensity was set at 70db SPL. The sounds were generated using MATLAB and played through an external soundcard (Fireface UCX) using the Psychtoolbox. In accordance with the international 10-5 system (extending the 10–20 system), EEG was recorded using 128 active Ag-AgCl electrodes (SynampsRT, Compumedics, France) for patients 2–4, and 64 electrodes for patient 1. Two of the electrodes served as ground (AFz) and reference (FCz). The EEG signal was recorded at 2 kHz sampling rate for patients 2–4, and at 1 kHz for patient 1. All electrodes were mounted on an electrode cap placed on the participant's head (Easycap, Germany). EEG was recorded twice for each patient, once with DBS ON (stimulation according to the usual clinical configuration described in Table 1) and once with DBS OFF. For each EEG recording, we recorded at least 5 min of rest, then we recorded with ASSR at 20 Hz, 40 Hz and then 80 Hz, 5 min each. During the setup of the EEG for each participant, DBS was turned off to allow for any washout effects to disappear (15–30 min, see Refs. 27). Next, the auditory experiment was performed during DBS OFF, after which brain stimulation was turned on, the data quality of the EEG checked and the auditory experiment repeated. Auditory stimuli were chosen at frequencies below 100 Hz to ensure that the expected phase-locked ASSRs would not be limited to the thalamus and the brainstem, but also extend to the primary auditory cortex.[28] Performing the

Table 1. Patient DBS stimulation details. Device type: type of stimulation device (implantable pulse generator). Age: each patient's age at the time of the experiment. PD duration: number of years elapsed since the initial diagnosis at the time of the experiment. Time since DBS: numbers of years elapsed since DBS implantation at the time of the experiment. Electrode configuration: $L$ =left electrode; $R$ =right electrode; all DBS leads are *Medtronic 3389*; numbers identify contacts on the leads ($L$ 2,3 and $R$ 10,11 are the most proximal contacts in each lead); + and 7 − indicate whether the contact is used as positive or negative pole in the stimulation; the absence of a "+" pole implies that the positive pole is the stimulator i.e. the electrode applies monopolar stimulation; all patients have monopolar montages. Amplitude: stimulation current/voltage of each electrode. Frequency: frequency of the stimulation signal's pulse PW=pulse width. LEDD=Levodopa equivalent daily dosage, an equivalent of the total daily dose of medication calculated by converting all medication into an equivalent dose of levodopa. This conversion is based on the work of Tomlinson *et al.*[25]

| Patient | Device type | Age (years) | PD duration (years) | Time since DBS (years) | Electrode config | Amplitude (Volt or mAmp) | Frequency (Hz) | PW ($\mu s$) | LEDD |
|---|---|---|---|---|---|---|---|---|---|
| 1 | Medtronic | 54 | 19 | 8 | L 2- | 3.2 V | 130 | 90 | 300 |
| | | | | | R 11+9−10- | 4.5 V | 130 | 90 | |
| 2 | Medtronic | 63 | 17 | 5 | L 2-3- | 3 V | 130 | 60 | 200 |
| | | | | | R 10-11- | 1.4 V | 130 | 60 | |
| 3 | Abbott | 56 | 11 | 1 | L 2- | 2 mA | 130 | 60 | 350 |
| | | | | | R 10- | 1.7 mA | 130 | 60 | |
| 4 | Medtronic | 53 | 9 | 3 | L 2- | 3.4 V | 130 | 60 | 0 |
| | | | | | R 10- | 3.7 V | 130 | 60 | |
| 5 | Abbott | 60 | 13 | 1 | L 2-3- | 3.2 mA | 160 | 40 | 200 |
| | | | | | R 10- | 3.2 mA | 130 | 60 | |

Int. J. Neur. Syst. 2025.35. Downloaded from www.worldscientific.com
by KATHOLIEKE UNIVERSITEIT LEUVEN on 12/23/25. Re-use and distribution is strictly not permitted, except for Open Access articles.

experiment with 3 different frequencies allows to show consistency in the results and were chosen similar to the work of Farahani *et al.*[26,22] A cohort of 5 age-matched healthy controls ($60 \pm 6$ years) is recorded with the same set-up. As analyses revealed that the number of electrodes did not affect the SNR of ASSRs down to 34 electrodes, we have recorded the healthy controls with the M24 EEG montage.

### 2.3. *Preprocessing*

The processing steps described in this paragraph are applied to the raw EEG data and are inspired by the PREP pipeline proposed by Bigdely-Shamlo *et al.*[29] Power line noise is removed using a 2 Hz-wide fourth-order zero-phase Butterworth notch filter centered at 50 Hz. The frequency range of interest is extracted using a bandpass fourth-order Butterworth filter between 1 Hz and 200 Hz. Bad channels are removed based on inter-channel variance, for each recording individually. Hereto each channel's internal variance is computed across the whole time series. The channels exhibiting high variance with respect to the others are marked as bad and removed. The channel removal outputs are then inspected visually. After removing these channels, there remains on average $55 \pm 4$, $117 \pm 7$, $117 \pm 5$, $118 \pm 5$, and $118 \pm 3$ for patients 1–5, respectively. Channels are re-referenced offline to a common average reference (CAR) both before and after bad channel identification. The preprocessing implementation relies on the fieldtrip toolbox.[30] It is well established that DBS introduces artifacts into EEGs.[21] Two options exist to deal with such artifacts: removing them from the data, or circumventing them. Popular methods to remove DBS artifacts are ICA.[31] and Hampel filtering[20] It is not trivial to remove DBS artifacts, as both methods inevitably affect signal characteristics. To investigate the extent of this effect, we compare ASSRs estimated with and without prior Hampel filtering of the data. Many EEG analyses including DBS do not attempt to remove artifacts, or simply low-pass filter the EEG recordings to avoid the main artifact components.[21] In our analyses, we require only to extract accurate estimates of ASSR intensities. By definition, an ASSR is a neural response occurring at the exact auditory stimulation frequency, i.e. 20 Hz, 40 Hz, and 80 Hz in our experiment. Prior to our analysis, we clearly identify the effect of DBS artifacts in our data to ensure they do not affect our estimated ASSR intensities in any way. To that end, we compute power spectra of whole EEG recordings with the multi-taper method applied to the fast Fourier transform (*ft_freqanalysis* from https://www.fieldtriptoolbox.org). The spectra range between 1 Hz and 90 Hz with a resolution of 0.01 Hz. We compute the power spectrum of each patient's recording in each configuration individually and per channel. For each configuration, we average the power spectra across channels, then across patients.

### 2.4. *ASSR estimation*

While various methods to estimate ASSR amplitudes exist, most share the same conceptual basis of estimating signal power at the frequency of auditory stimulation. In its simplest form, ASSR amplitudes can be estimated by computing the summed squares of the Real and Imaginary parts of the fast Fourier transform (FFT) of EEG recordings across electrodes. The estimated ASSR is then the frequency bin of the resulting power spectrum which contains the auditory stimulus frequency.[32] A more elaborate alternative is to bandpass filter the EEG recording around the frequency of auditory stimulation, to split it into shorter time segments, and to average them before computing the FFT.[33] However, both methods rely on the explicit computation of power spectra, the resolution of which affects the estimated ASSRs. We propose an alternative which estimates ASSRs at the exact frequency of interest without such a step, avoiding the resolution dependency as a result. The method's steps are illustrated in Fig. 1 and is described next. We record EEGs as described in Sec. 2.2 both at rest and with auditory stimuli modulated at 20 Hz, 40 Hz, and 80 Hz. Each 5 min-long recording is split into 30 trials of 10 s each. We compute the correlation of each trial to ASSR templates at the frequency of interest via a popular method from the brain-computer interface (BCI) literature. In that field, the method is used to identify mentally selectable targets from periodic brain responses in EEGs.[34–37] It consists of comparing the EEG trial ($X$) with a matrix ($Y$) of sines and cosines at the ASSR frequency of interest via canonical correlation analysis (CCA). It optimizes kernels $a$ and $b$ to maximize the correlations $\rho$ between the canonical projections of $X$ and $Y$: $U = Xa$ and

Int. J. Neur. Syst. 2025.35. Downloaded from www.worldscientific.com
by KATHOLIEKE UNIVERSITEIT LEUVEN on 12/23/25. Re-use and distribution is strictly not permitted, except for Open Access articles.

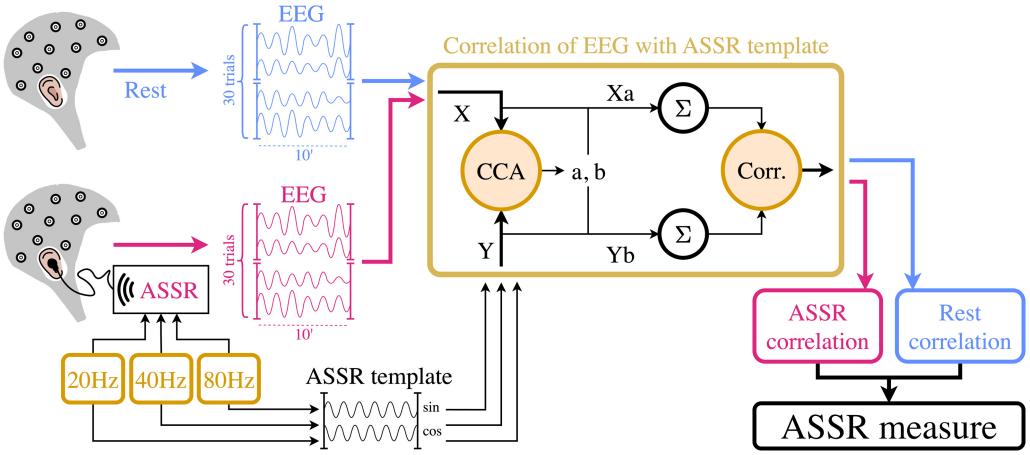



Fig. 1. ASSR estimation pipeline from EEGs. ASSR: auditory steady-state response; EEG: electroencephalography; CCA: canonical correlation analysis; $\sum$: sum across channels; Corr.: Pearson correlation.

$V = Yb$. Let $\rho^*$ be the optimized correlation for $X$ and $Y$, $\Sigma_{XY}$ the covariance between $X$ and $Y$, $\Sigma_X$ and $\Sigma_Y$ the variances of $X$ and $Y$, respectively.

$$\rho^* = \max_{a,b}\left(\mathrm{corr}(U,V)\right) = \max_{a,b}\left(\frac{a^T\Sigma_{XY}b}{\sqrt{a^T\Sigma_X a}\sqrt{b^T\Sigma_Y b}}\right).$$

The canonical EEG segment ($U$) and canonical ASSR template ($V$) are each summed across channels. The sums are Pearson correlated to yield a single output for each trial. The method ensures that the output correlation is proportional to the intensity of ASSRs at the frequency of interest. Note that the output correlations relate to the trial's EEG power at the frequency of the templates since the sum of the squared coefficients, obtained by multiplying sines and cosines with a signal, returns the power of the corresponding Fourier component. This entails that the output correlations are driven by all brain activity and noise at the frequency of interest, thereby reflecting more than just ASSRs. To factor out all confounding activity, we baseline the output correlations of trials during auditory stimuli ($U^{\mathrm{assr}}$, $V^{\mathrm{assr}}$) with resting state output correlations ($U^{\mathrm{rest}}$, $V^{\mathrm{rest}}$). Let $\mathrm{corr}(A, B)$ be the Pearson correlation of $A$ with $B$, $U_i$ the $i$th channel of canonical EEG segment $U$, and $V_i$ the $i$th channel of canonical ASSR template $V$:

$$\mathrm{ASSR} = \frac{\mathrm{corr}\left(\sum_i U_i^{\mathrm{assr}}\ ,\ \sum_i V_i^{\mathrm{assr}}\right)}{\mathrm{corr}\left(\sum_i U_i^{\mathrm{rest}}\ ,\ \sum_i V_i^{\mathrm{rest}}\right)}.$$

This procedure provides a reliable measure of ASSR intensity within each EEG trial. We apply this process to each recorded condition to obtain 20 Hz, 40 Hz, and 80 Hz ASSR intensity measures during DBS ON and OFF for 30 trials per patient.

### 2.5. *Signal-to-noise ratio*

In our experiment, we have recorded Parkinson patients with high-density EEG montages, i.e. Easycap M15 (128 channels) and M64 (64 channels). Placing such a number of electrodes is a long process which makes the recording demanding for the patient. As such, we investigated how the electrode montage affects the ASSR estimation with our method. To do so, we estimate the ASSRs signal-to-noise ratio (SNR) from the recordings:

$$\mathrm{SNR} = \frac{\mathrm{ASSR}}{\sigma_{noise}},$$

where $\sigma_{\mathrm{noise}}$ is the standard deviation of noise estimations ($n_j$). Panel A of Fig. 3 illustrates the process to estimate ASSRs SNR from a recording. It consists of first estimating the ASSR at the auditory stimulation frequency ($fs$). To estimate the noise variation, we apply the ASSR estimation procedure at frequencies surrounding $fs$, where no auditory stimulation is applied ($n_j$). Noise estimates are spaced by 0.5 Hz, ranging from $[fs-4\ ;\ fs+4]$ Hz. To ensure the $fs$ Hz auditory stimulation does not affect the noise estimates, they are not estimated at frequencies within $[fs-1.5\ ;\ fs+1.5]$ Hz. From our high-density electrode montage (Easycap M15), we filter out submontages of electrodes before estimating

Int. J. Neur. Syst. 2025.35. Downloaded from www.worldscientific.com
by KATHOLIEKE UNIVERSITEIT LEUVEN on 12/23/25. Re-use and distribution is strictly not permitted, except for Open Access articles.

ASSRs from the remaining channels. We consider submontages yielding 64 channels (Easycap M64), 34 channels (Easycap M24), and a subset of the M64 montage centered around the auditory cortex yielding 18 channels (P7, P8, TP9, TP7, TP8, TP10, T7, C5, C6, T8, FT9, FT7, FC5, FC6, FT8, FT10, F7, F8). Estimating the SNR of ASSRs further provides a metric to compare our CCA-based method to other ASSR estimation methods. As the SNR is proportional to the ASSR itself, a higher SNR indicates a more prominent ASSR. We compare the performance of the CCA-based method with the power,[32] and the averaging[33] methods introduced in Sec. 2.4 both with the M24 and the auditory montages.

### 2.6. *Statistical testing*

Statistical tests were employed to compare distributions of ASSRs and SNRs throughout our work. One-way ANOVAs were used for trial based comparisons such as SNR with respect to electrode montage, SNR across estimation method, and the effect of DBS on ASSRs within each patient. The effects of DBS and PD on ASSRs at the group level were evaluated by fitting linear mixed effect models to account for inter-patient variability. The models estimating the effect of DBS within groups of PD patients were designed with ASSR as response variable, DBS as fixed effect, and participant identifier as grouping variable ($ASSR \sim DBS + (1|participant)$). The models estimating the effect of PD on ASSRs both with and without DBS were designed with ASSR as response variable, PD-HC group as fixed effect, and participant identifier as grouping variable ($ASSR \sim group + (1|participant)$). Participants from the healthy and PD cohorts were attributed distinct identifiers. Each group of statistical tests was corrected for multiple testing with the false detection rate (FDR) procedure (Benjamini and Hochberg[38]).

### 2.7. *Tools*

All processing, analyses and statistical tests were run with the Matlab R2024b Software (https://www.mathworks.com). The preprocessing and most analyses described in the Methods section rely on the fieldtrip toolbox (https://www.fieldtriptoolbox.org) developed by Oostenveld *et al.*[30] Figure 1 was created with the *draw.io* software (https://www.drawio.com). Figures 2 and 3 were generated with Matlab R2024b Software (www.mathworks.com).

## 3. Results

### 3.1. *DBS artifacts*

Figure 2(a) shows that DBS artifacts do not affect ASSR measures from our data at the frequencies of interest. The first row of power spectra (Fig. 2(a) DBS OFF) confirms the presence of ASSRs at 20 Hz, 40 Hz, 80 Hz during auditory stimulation, and their absence during rest (baseline). The second row (Fig. 2(a) DBS ON) reveals sporadic DBS artifacts, occurring at narrow-band frequencies. These artifacts prove consistent across auditory stimulation and resting conditions. The power spectra in the third row (Fig. 2(a) DBS ON - ZOOM) focuses on the corresponding frequency of interest. It confirms that DBS artifacts do not overlap with ASSRs. These findings give confidence that 20 Hz, 40 Hz, and 80 Hz ASSRs can be measured accurately in DBS ON condition. To investigate the extent to which DBS artifact cleaning can affect the estimated ASSRs, we apply Hampel filtering to the data before ASSR estimation. Figure 2(b) shows that such filtering cleanly removes the DBS artifacts across all frequencies, leaving the ASSR frequency seemingly unaffected. Note that in the Hampel filtering procedure, the more outliers are detected, the more the signal is filtered. Figure 2(c) reveals that estimated ASSRs are affected by the Hampel filtering of DBS artifacts (DBS ON), and are hardly affected in their absence (DBS OFF). Hampel filtering trims artifact peaks throughout the power spectrum and projects the signal back to the time domain with conserved overall power. Signals during DBS have more artifacts, and as such, its nonartifactual frequencies are heightened. It explains the increase in ASSR by Hampel filtering of the signal during DBS. Such an increase does not represent an inherent feature of the signal but is rather a consequence of its processing. To avoid this bias, we do not apply the Hampel filter to the data before estimating ASSRs.

### 3.2. *CCA-based method validation*

Figure 3(b) shows that ASSR estimation remains similar across EEG montages ranging from 128 to 34

Int. J. Neur. Syst. 2025.35. Downloaded from www.worldscientific.com
by KATHOLIEKE UNIVERSITEIT LEUVEN on 12/23/25. Re-use and distribution is strictly not permitted, except for Open Access articles.

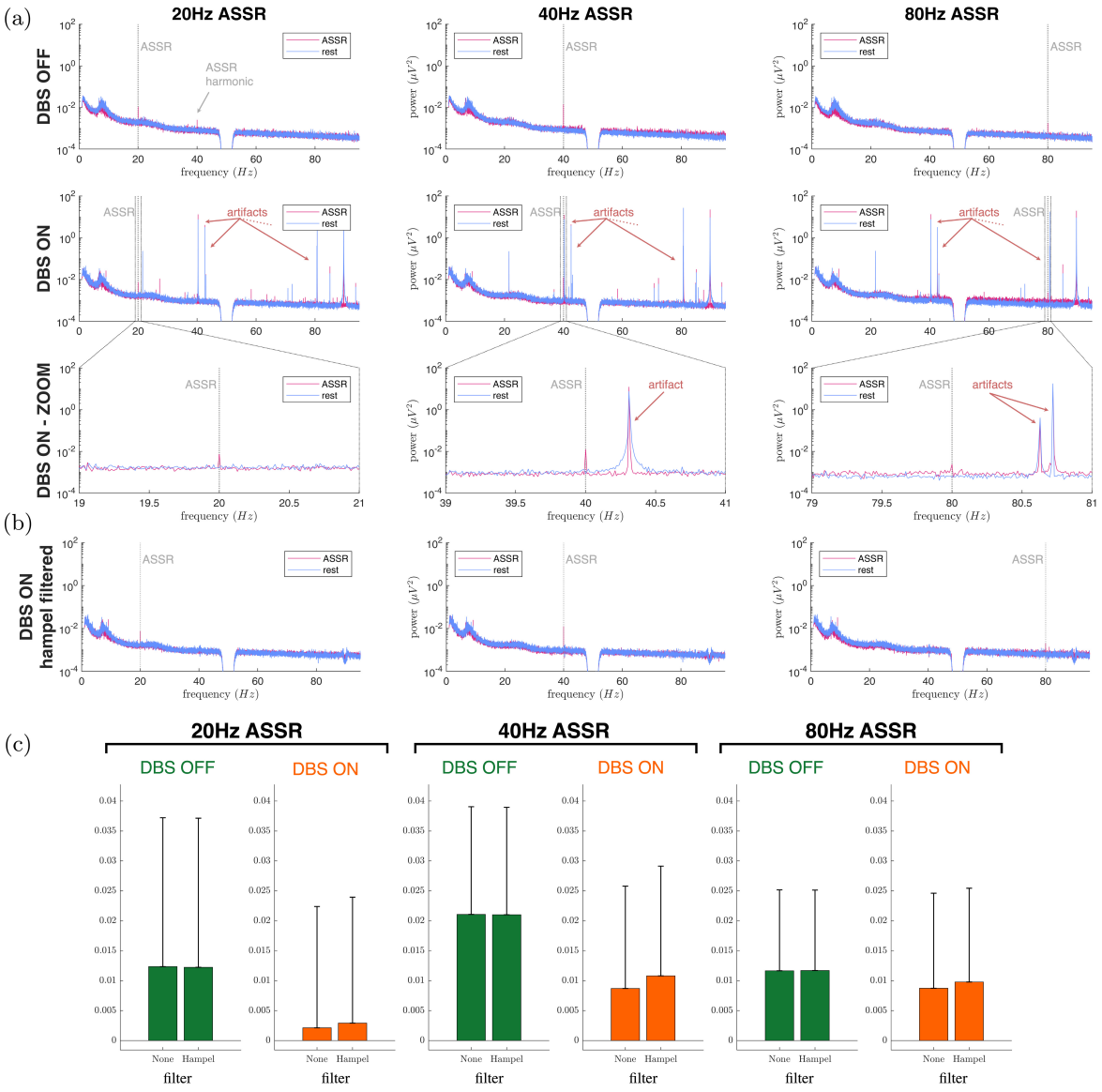



Fig. 2. (a) Power spectral densities (PSD) of PD patients at rest (baseline) and during 20 Hz-, 40 Hz-, and 80 Hz-modulated auditory stimulation (ASSR). First row: DBS is turned OFF for the patients. Second row: DBS is turned ON for the patients. Third row: zoom on the auditory stimulated frequency with DBS turned ON for the patients. (b). PSD of PD patients at rest (baseline) and during 20 Hz-, 40 Hz-, and 80 Hz-modulated auditory stimulation (ASSR) with DBS turned ON and after Hampel filtering of the DBS artifacts.[20] (c) Comparison of the ASSR distributions estimated from unfiltered and Hampel filtered EEG recordings in both the presence and absence of DBS artifacts.

channels both in DBS OFF ($F(3,56) = 0.10$, $p = 0.962$) and DBS ON conditions ($F(3,56) = 0.24$, $p = 0.869$). SNRs prove to be higher overall in the absence of DBS, and with more variability, regardless of the EEG montage (Fig. 3(b)) or the estimation method (Fig. 3(c)). Figure 3(c) reveals that the CCA-method extracts ASSRs with higher SNR on average than the power-method, though not significantly (DBS OFF: $F(1,28) = 0.82, p = 0.374$; DBS ON: $F(1,28) = 1.27$, $p = 0.268$). On average, the CCA-method yields SNRs similar to the average-method (DBS OFF: $F(1,25) = 0.00, p = 0.961$; DBS ON: $F(1,25) = 0.12, p = 0.735$). On average, the power-method yields lower SNRs than the average-method, though not significantly either (DBS OFF: $F(1,25) = 1.00$, $p = 0.328$; DBS ON: $F(1,25) = 1.71, p = 0.202$).

Int. J. Neur. Syst. 2025.35. Downloaded from www.worldscientific.com
by KATHOLIEKE UNIVERSITEIT LEUVEN on 12/23/25. Re-use and distribution is strictly not permitted, except for Open Access articles.

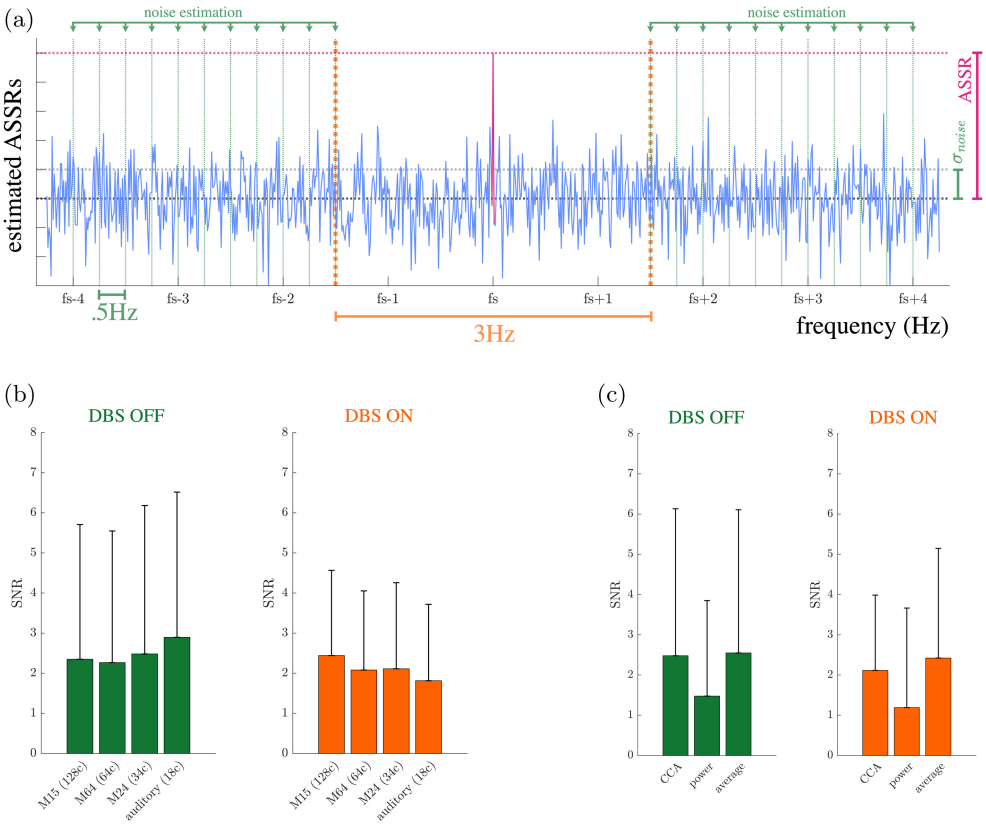



Fig. 3. (a) Illustration of the scheme to estimate ASSR SNR. It depicts 16 Hz of ASSR centered on the auditory stimulation frequency (*Fs*). (b) SNRs of ASSRs estimated with the CCA-based method considering electrode montages yielding decreasing numbers of channels. Electrode montages are the Easycap M15 (128 channels), M64 (64 channels), M24 (34 channels) and an auditory subset of electrodes extracted from the M64 montage (18 channels). (c) SNRs of ASSRs estimated with different methods (CCA-based, power,[32] averaging[33]) from M24 EEG electrode montage (34 channels).

### 3.3. *ASSRs*

Figure 4 shows distributions of 20 Hz, 40 Hz, and 80 Hz ASSR measures across trials in the presence and absence of DBS. At 20 Hz, patient 2 ($F(1,58) = 6.71$, $p = 0.030$), patient 3 ($F(1,58) = 5.09, p = 0.048$) and patient 5 ($F(1,58) = 9.84$, $p = 9.9e-3$) show significantly lower ASSR during DBS. All three patients show medium effects (P2: Cohen's $d = 0.660$ [0.144, 1.171]; P3: Cohen's $d = 0.575$ [0.062, 1.083]; P5: Cohen's $d = 0.799$ [0.276, 1.316]). At 40 Hz, patient 1 ($F(1,58) = 6.15$, $p = 0.034$), patient 2 ($F(1,58) = 9.40$, $p = 9.9e-3$), patient 3 ($F(1,58) = 5.03$, $p = 0.048$), and patient 4 ($F(1,58) = 11.38, p = 6.6e-3$) have significantly lower ASSR in DBS ON condition. Effects are moderate to strong for the four patients (P1: Cohen's $d = 0.632$ [0.117, 1.142]; P2: Cohen's $d = 0.781$ [0.259, 1.297]; P3: Cohen's $d = 0.571$ [0.059, 1.079]; P4: Cohen's $d = 0.860$ [0.333, 1.380]). At 80 Hz, patient 1 ($F(1,58) = 14.73$, $p = 2.3e-3$) and patient 5 ($F(1,58) = 19.52, p = 6.6e-4$) show a significant reduction in ASSR during DBS, with strong effect (Cohen's $d = 0.978$ [0.444, 1.504]; Cohen's $d = 1.126$ [0.582, 1.661]). At the group level, mixed effect models of each ASSR frequency of interest reveal a significant main effect of DBS on 20 Hz ASSR ($\beta = -0.0092$, $SE = 0.0024$, $p = 1.9e-4$), 40 Hz ASSR ($\beta = -0.0092$, $SE = 0.0016$, $p = 2.6e-8$) and 80 Hz ASSR ($\beta = -0.0052$, $SE = 0.0014$, $p = 2.0e-4$). The effect size of DBS on group ASSR distributions is moderate for all frequencies (20 Hz: Cohen's $d = 0.423$ [0.194, 0.651]; 40 Hz: Cohen's $d = 0.496$ [0.266, 0.725]; 80 Hz: Cohen's $d = 0.347$ [0.120, 0.575]). Overall, all significant comparisons between DBS ON and OFF show a reduction of ASSR by DBS at all three frequencies of interest.

We can compare the group ASSR distributions of healthy age-matched controls (HC) with those of the

Int. J. Neur. Syst. 2025.35. Downloaded from www.worldscientific.com
by KATHOLIEKE UNIVERSITEIT LEUVEN on 12/23/25. Re-use and distribution is strictly not permitted, except for Open Access articles.

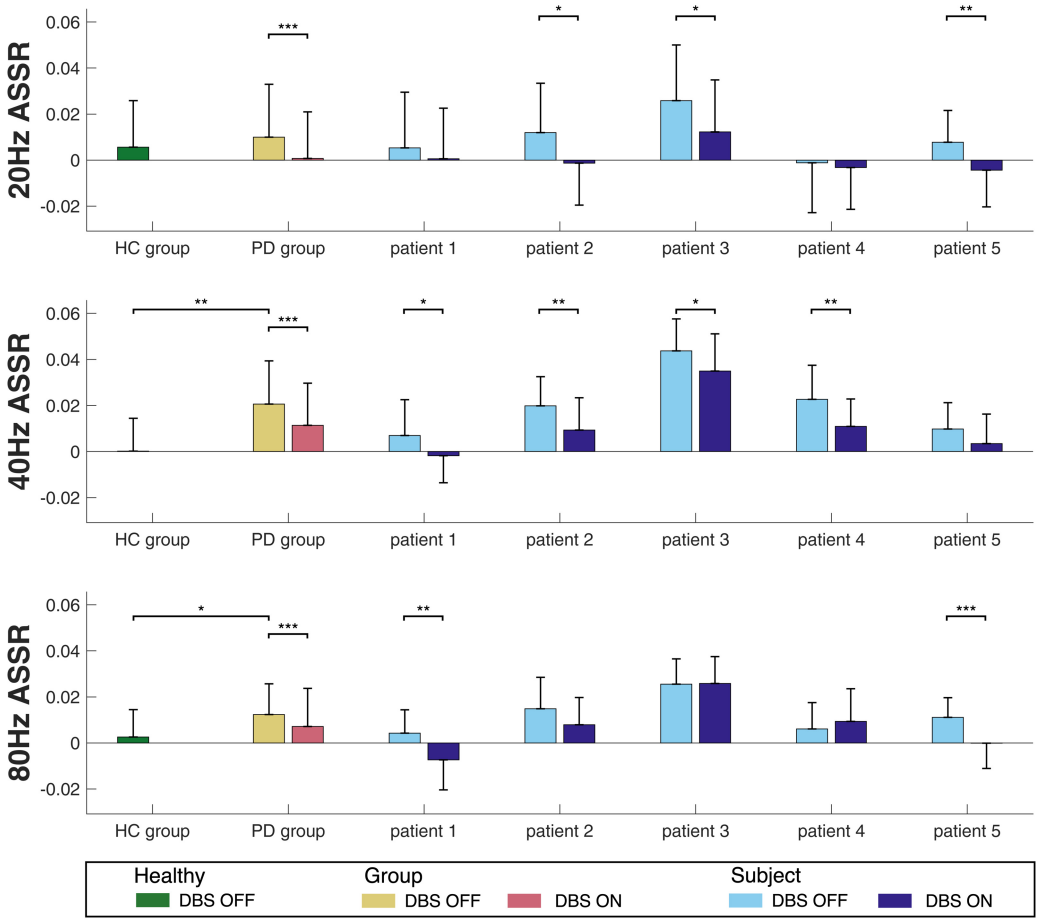



Fig. 4. Group- and patient-wise distributions of 20 Hz, 40 Hz, 80 Hz auditory steady state responses (ASSR) in DBS ON (right) and OFF (left) conditions. ASSRs were estimated by the CCA-based method described in Fig. 1, with Easycap M24 montage (34 channels). A negative ASSR indicates that the baseline signal correlates more with the ASSR template than during auditory stimulation. Bars represent the average of each distribution, while whiskers depict their standard deviation. Stars displayed above DBS ON-OFF distributions indicate the significance level of DBS in explaining the variance in the corresponding ASSR distribution. Stars displayed above the healthy control (HC) group indicate the significance level of the pathology (PD with DBS ON/OFF) in explaining the variance in the corresponding ASSR distribution. Subject-wise significance levels were evaluated with one-way ANOVAs and group-wise significance levels were evaluated with linear mixed effects models. All significances were corrected for multiple comparisons (Benjamini and Hochberg[38]). Basic significance levels are (*: $p < 0.05$, **: $p < 0.01$, ***: $p < 0.001$). Each patient distribution is made up of 30 trials. PD and HC group distributions are made up of 150 trials.

PD cohort (PD group). Figure 4 shows that 20 Hz ASSRs prove to be lower on average than the PD group without DBS, and higher than the PD group with DBS, though we report no significant effect of PD on 20 Hz ASSR. At 40 Hz, ASSRs of the HC group are lower than the PD group without DBS ($\beta = -0.0204$, $SE = 0.0061$, $p = 2.7e-3$) and insignificantly lower than the PD group with DBS. The effect of PD on 40 Hz ASSR without DBS is a strong increase (Cohen's $d = -1.220$ [$-1.465$, $-0.973$]), and its effect on 40 Hz ASSR with DBS is reduced to a moderate increase (Cohen's $d = -0.678$ [$-0.910$, $-0.446$]). At 80 Hz, ASSRs of the HC group are similarly lower than the PD group without DBS ($\beta = -0.0098$, $SE = 0.0040$, $p = 0.020$) and insignificantly lower with DBS. Much like at 40 Hz, the effect of PD on 80 Hz ASSR without DBS is a strong increase (Cohen's $d = -0.775$ [$-1.009$, $-0.540$]), and its effect on 40 Hz ASSR with DBS is reduced to a moderate increase (Cohen's $d = -0.317$ [$-0.544$, $-0.090$]).

Int. J. Neur. Syst. 2025.35. Downloaded from www.worldscientific.com
by KATHOLIEKE UNIVERSITEIT LEUVEN on 12/23/25. Re-use and distribution is strictly not permitted, except for Open Access articles.

## 4. Discussion

Literature reports that PD patients experience significant impairments relating to central auditory processing such as hearing loss,[12] speech discrimination,[11] altered deviance in discriminating basic auditory features, and selective auditory attention.[13] For PD patients whose motor symptoms are treated by DBS, stimulation was shown to have an effect on auditory processing as observed in multiple studies. For instance, DBS was shown to modulate both auditory- and somatosensory processing-related evoked potentials in patients with advanced PD.[8] DBS was also shown to modulate cortical auditory processing in auditorily-evoked responses.[10] These studies focus on evoked potentials in the cortex but, as central auditory processing also involves deep sources, the effect of DBS on auditory processing remains elusive. Previous research showed activity in the STN evoked by auditory stimuli in the form of standard and deviant syllables in both attentive and pre-attentive modes.[18] It essentially means that STN is involved in auditory processing which could explain why STN-DBS modulates auditory processing. Furthermore, while the mechanism of DBS is still under debate, a large body of evidence suggests that DBS exerts a widespread effect on neural activity by modulating brain networks, which can indirectly modulate auditory processing.[39,40] We proposed a new angle by studying the effect of DBS by involving spectral responses rather than cortical evoked potentials. Additionally, our research leverages ASSR which involves both deep (auditory brainstem) and cortical (primary auditory cortex) sources.[22]

To investigate ASSRs from EEG, we propose a method based on canonical correlation analysis inspired from brain–computer interface literature. We investigated whether the estimated ASSRs depend on the electrode montage. Results show that ASSRs SNR are similar for 128, 64, 34 electrodes, and a subset of 64 electrodes targeted on the auditory cortex totaling 18 electrodes. This result implies that a montage with as low electrode density as 34 electrodes (Easycap M24) is sufficient to estimate ASSRs with the method we propose. We have compared our CCA-based method to methods used in previous works. Our results indicate that the CCA-based method extracts ASSRs with higher SNR than the power method, and similar SNR to the average method. The CCA-based method, though yielding ASSRs with SNRs similar to the averaging method, does not rely on explicit power computation, and does not in turn depend on the spectrum's resolution.

Our analyses were performed on three distinct ASSR frequencies: 20 Hz, 40 Hz and 80 Hz. Distributions at patient level present some variability both across patients and frequencies. For instance, patient 3 has stronger ASSRs across all frequencies, while patient 1's ASSRs are weaker overall. The effect of DBS on ASSRs is more consistent: all significant distribution comparisons present a decrease in ASSR intensity during DBS. In fact, all but one distribution comparison show a decrease in ASSR during DBS. The exception lies in patient 4 during 80 Hz ASSR, which shows a (nonsignificant) increase during DBS. Such a difference could be connected to an inherent difference in neuronal background noise, or be due to the fact that patient 4 is the only one not supplementing DBS with medication. Dopaminergic medication was previously shown to affect auditory temporal processing, though less than by STN-DBS.[41] Furthermore, group level distributions show significant reductions of 20 Hz, 40 Hz and 80 Hz ASSR in the presence of DBS. This supports the hypothesis that DBS modulates ASSRs, at least at those frequencies. Overall, our results support the hypothesis that DBS modulates auditory processing, and suggest the effect could be inhibitory.

While our results suggest an effect of DBS on ASSR, they lead to a more important question: *What is the nature of the impact of DBS on the physiology of auditory processing?* Related works can aid in developing an answer. First, previous works indicate that the STN does not project to the auditory cortex via direct pathways.[42,43] Recent research on mice suggests the existence of an auditory cortico-basal ganglia loop.[44,45] Additionally, it was shown that the STN plays a role in auditory processing [18] as well as in language processing.[46] Work from Hnazaee *et al.*[19] (co-author of this paper) highlights local frequency following responses (akin to ASSRs) in the STN. It strongly indicates that the STN is directly engaged in auditory processing by interaction with the inferior colliculus of the brainstem. As a result, stimulation of the STN likely affects neural responses to sound via the brainstem. Unpublished results from Santens' group (co-author of this paper) suggest that

Int. J. Neur. Syst. 2025.35. Downloaded from www.worldscientific.com
by KATHOLIEKE UNIVERSITEIT LEUVEN on 12/23/25. Re-use and distribution is strictly not permitted, except for Open Access articles.

STN activity in auditory processing is probably related to the gating of salient stimuli. Santens *et al.*'s work concerns research of STN local field potentials (**LFP**) in attentive discrimination (P300-like) and nonattentive discrimination (Mismatch Negativity-like) of speech sounds (phonological stimuli) and nonspeech tones. Time-locked spectral alterations in the STN were only found in attentive discrimination paradigms but were similar for speech and nonspeech stimuli. This indicates a role of the STN in attentive discrimination of auditory stimuli, but not restricted to speech sounds. This suggests that STN is involved in the detection of salient stimuli that are not specific to speech. In that context, STN stimulation might be able to affect the gating of incoming stimuli which would explain that STN-DBS modulates ASSRs. Further research is needed to elucidate the nature of this effect. Moreover, the above-mentioned time-locked spectral alterations in the STN were shown to occur long before cortical responses are detected. The authors suspect that signaling in the STN is coming from connections with the reticular system (e.g. pedunculopontine nucleus) that relays towards the STN in order to prepare for cortical processing and/or switch between automatic and nonautomatic behavioral responses. Investigating the connectivity between the STN and the brainstem would provide evidence for the hypothesis and could be the subject of further research.

In our analyses, we compare ASSRs of the PD cohort with and without DBS to age-matched healthy controls. Those results suggest that PD pathologically increases ASSRs in patients (at least at 40 Hz and 80 Hz), which DBS reduces towards healthy levels. These results indicate that the modulation of auditory processing by STN-DBS could potentially be beneficial to PD patients. Future research including behavioral measures of auditory perception could clarify whether that is the case. This raises the question of whether DBS can be beneficial to other groups, for instance patients with auditory dysfunctions. Concretely, extending our results to an interpretation of the effect of either PD pathology or STN-DBS on the physiology of auditory processing would require further research including more participants. An interesting extension would also be to assess the location of the electrodes more precisely within the STN, for instance by merging computerized tomography (CT) with MRI. Formal symptomatic evaluations (UPDRS scores) of the participants and audition related screening, e.g. similar to the work of Bidelman,[28] would also be useful to make sense of inter-patient variability in ASSRs.

Other prospects for further research could be to study the influence of the frequency of the ASSRs on the modulation. Indeed, it is generally accepted that ASSRs at different frequencies have varying intensities.[47] For instance, 40 Hz ASSRs are known to be particularly strong, to the extent that they are considered a candidate noninvasive biomarker for multiple neuropsychiatric disorders.[48] The stimulation frequencies used in the experiment are harmonics. They are suited for showing that modulation by DBS exists but are limited in their ability to dissect the nature of the effect along the auditory spectrum. One instance in which DBS might affect ASSRs differently depending on the auditory stimulation frequency holds on the premise that central auditory processing involves both cortical and subcortical sources. ASSRs are phase-locked responses and as 200 Hz is the upper limit above which there is no phase-locking in the cortex,[28] ASSRs above that frequency would take source exclusively from subcortical sources. As such, repeating the experiment with ASSRs above 200 Hz is expected to yield different results since DBS might affect subcortical sources differently from cortical sources. However, whether it would be possible to record with EEGs is another challenge considering the low SNR and potential closed fields of subcortical sources. More generally, repeating the experiments in more varied frequency configurations could yield insights into the extent to which the effect of DBS depends on auditory stimulation frequency.

## 5. Conclusion

We have leveraged EEG to estimate the intensity of ASSR in 5 PD patients in the presence and absence of subthalamic nucleus DBS. Comparing the ASSRs suggests that they are modulated by DBS. Our results further indicate that the modulation is in the form of a reduction in ASSR intensity. Comparing the patients' ASSRs to those of an age-matched

Int. J. Neur. Syst. 2025.35. Downloaded from www.worldscientific.com
by KATHOLIEKE UNIVERSITEIT LEUVEN on 12/23/25. Re-use and distribution is strictly not permitted, except for Open Access articles.

healthy cohort suggests a pathological effect of PD on the auditory responses, which seems to be disrupted by DBS. The results support our hypothesis that STN-DBS modulates central auditory processing in PD. They pave the way for future research investigating how DBS affects the physiology of auditory processing, which could lead to improved DBS intervention and new auditory rehabilitation procedures.

## Acknowledgments

MF is supported by the Hermes Fund of the National Fund for Scientific Research Flanders (SB/151022). MMVH is supported by the research grants received from the European Union's Horizon 2020 research and innovation programme under grant agreement No. 857375, the special research fund of the KU Leuven (C24/18/098), the Belgian Fund for Scientific Research – Flanders (G0A4118N, G0A4321N, G0C1522N), and the Hercules Foundation (AKUL 043). AM is supported by the Belgian Fund for Scientific Research – Flanders (11P1G24N).

We would like to thank Tom Francart for suggesting the use of ASSRs and lending the auditory stimulation equipment. We would also like to thank the attendees of the Translational Neurophysiology lab meetings at UCL and in particular Bernadette Van Wijk and Vladimir Litvak for their insightful feedback.

## ORCID

Thomas Pirenne https://orcid.org/0000-0002-3121-7881
Mansoureh Fahimi Hnazaee https://orcid.org/0000-0001-6284-7723
Patrick Santens https://orcid.org/0000-0002-8886-9776
Aline Moorkens https://orcid.org/0000-0002-0304-0281
Marc M. Van Hulle https://orcid.org/0000-0003-1060-7044

## References

1. T. J. Hirschauer, H. Adeli and J. A. Buford, Computer-aided diagnosis of Parkinson's disease using enhanced probabilistic neural network, *J. Med. Syst.* **39** (2015) 179.
2. F. J. Martinez-Murcia, J. E. Arco, C. Jimenez-Mesa, F. Segovia, I. A. Illan, J. Ramirez and J. M. Gorriz, Bridging imaging and clinical scores in Parkinson's progression via multimodal self-supervised deep learning, *Int. J. Neural Syst.* **34** (2024) 2450043.
3. S. Bhat, U. R. Acharya, Y. Hagiwara, N. Dadmehr and H. Adeli, Parkinson's disease: Cause factors, measurable indicators, and early diagnosis, *Comput. Biol. Med.* **102** (2018) 234–241.
4. S. Chiken and A. Nambu, Mechanism of deep brain stimulation, *Neuroscientist* **22** (2016) 313–322.
5. L. H. Levinson, D. J. Caldwell, J. A. Cronin, B. Houston, S. I. Perlmutter, K. E. Weaver, J. A. Herron, J. G. Ojemann and A. L. Ko, Intraoperative characterization of subthalamic nucleus-to-cortex evoked potentials in Parkinson's disease deep brain stimulation, *Front. Human Neurosci.* **15** (2021) 590251.
6. A. Priori, C. Cinnante, S. Genitrini, A. Pesenti, G. Tortora, C. Bencini, M. V. Barelli, V. Buonamici, F. Carella, F. Girotti, P. Soliveri, F. Magrini, A. Morganti, A. Albanese, S. Broggi, G. Scarlato and S. Barbieri, Non-motor effects of deep brain stimulation of the subthalamic nucleus in Parkinson's disease: Preliminary physiological results, *Neurolog. Sci.* **22** (2001) 85–86,rResults.
7. A. Conte, N. Modugno, F. Lena, S. Dispenza, B. Gandolfi, E. Iezzi, G. Fabbrini and A. Berardelli, Subthalamic nucleus stimulation and somatosensory temporal discrimination in Parkinson's disease, *Brain* **133** (2010) 2656–2663.
8. K. Airaksinen, J. P. Mäkelä, S. Taulu, A. Ahonen, J. Nurminen, A. Schnitzler and E. Pekkonen, Effects of DBS on auditory and somatosensory processing in Parkinson's disease, *Human Brain Mapping* **32** (2011) 1091–1099.
9. B. H. Bahners, E. Florin, J. Rohrhuber, H. Krause, J. Hirschmann, R. van de Vijver, A. Schnitzler and M. Butz, Deep brain stimulation does not modulate auditory-motor integration of speech in Parkinson's disease, *Front. Neurol.* **11** (2020) 655.
10. K. Valkonen, J. P. Mäkelä, K. Airaksinen, J. Nurminen, R. Kivisaari, H. Renvall and E. Pekkonen, Deep brain stimulation of subthalamic nucleus modulates cortical auditory processing in advanced Parkinson's Disease, *PLoS One* **17** (2022) e0264333.
11. C. Vitale, V. Marcelli, T. Abate, A. Pianese, R. Allocca, M. Moccia, E. Spina, P. Barone, G. Santangelo and M. Cavaliere, Speech discrimination is impaired in parkinsonian patients: Expanding the audiologic findings of Parkinson's disease, *Parkinson. Related Disorders* **22** (2016) S138–S143.
12. R. L. Folmer, J. J. Vachhani, S. M. Theodoroff, R. Ellinger and A. Riggins, Auditory processing abilities of Parkinson's disease patients, *BioMed Res. Int.* **2017** (2017) 1–10.

Int. J. Neur. Syst. 2025.35. Downloaded from www.worldscientific.com
by KATHOLIEKE UNIVERSITEIT LEUVEN on 12/23/25. Re-use and distribution is strictly not permitted, except for Open Access articles.

13. E. De Groote, K. De Keyser, A. Bockstael, D. Botteldooren, P. Santens and M. De Letter, Central auditory processing in parkinsonian disorders: A systematic review, *Neurosci. Biobehav. Rev.* **113** (2020) 111–132.
14. G. Galvez, M. Recuero, L. Canuet and F. Del-Pozo, Short-term effects of binaural beats on EEG power, functional connectivity, cognition, gait and anxiety in Parkinson's disease, *Int. J. Neural Syst.* **28**(5) (2018) 1750055.
15. D. Gonzalez, R. Bruna, J. C. Martinez-Castrillo, J. M. Lopez and G. D. Arcas, First longitudinal study using binaural beats on parkinson disease, *Int. J. Neural Syst.* **33**(6) (2023) 2350027.
16. D. Gonzalez, L. Sigcha, J. M. Lopez, C. Asensio, I. Pavon, N. Costa, S. Costa, M. Gago, J. C. Martnez-Castrillo and G. D. Arcas, Evolution of the motor symptoms in parkinson disease under auditory stimulation, *Int. J. Neural Syst.* **35**(7) (2025) 2550030.
17. A. Gómez-Rodellar, J. Mekyska, P. Gómez-Vilda, L. Brabenec, P. Simko and I. Rektorova, A pilot study on the functional stability of phonation in eeg bands after repetitive transcranial magnetic stimulation in parkinson's disease, *Int. J. Neural Syst.* **33**(6) (2023) 2350028.
18. M. De Letter, A. Aerts, J. Van Borsel, S. Vanhoutte, L. De Taeye, R. Raedt, P. van Mierlo, P. Boon, D. Van Roost and P. Santens, Electrophysiological registration of phonological perception in the subthalamic nucleus of patients with Parkinson's Disease, *Brain Lang.* **138** (2014) 19–26.
19. M. F. Hnazaee, H. Zhao, S. Hao, J. Huber, A. Moorkens, C. Lambert, S. Zhan, D. Li, B. Sun, V. Litvak and C. Cao, Generators of the frequency-following response in the subthalamic nucleus: Implications for non-invasive deep brain stimulation, *Brain Stimulation* **17**(4) (2024), 847–849.
20. A. L. Kandemir, V. Litvak and E. Florin, The comparative performance of DBS artefact rejection methods for meg recordings, *NeuroImage* **219** (2020) 117057.
21. G. Lio, S. Thobois, B. Ballanger, B. Lau and P. Boulinguez, Removing deep brain stimulation artifacts from the electroencephalogram: Issues, recommendations and an open-source toolbox, *Clin. Neurophysiol.* **129** (2018) 2170–2185.
22. E. D. Farahani, J. Wouters and A. Wieringen, Brain mapping of auditory steady-state responses: A broad view of cortical and subcortical sources, *Human Brain Mapping* **42** (2021) 780–796.
23. L. Wang, E. Noordanus and A. J. van Opstal, Estimating multiple latencies in the auditory system from auditory steady-state responses on a single EEG channel, *Sci. Rep.* **11** (2021) 2150.
24. S. V. Lier, K. Batens, P. Santens, D. V. Roost, M. V. Herreweghe and M. D. Letter, The influence of subthalamic nucleus stimulation on pragmatic language production in Parkinson's disease, *Acta Neurol. Belgica* **116** (2016) 163–170.
25. C. L. Tomlinson, R. Stowe, S. Patel, C. Rick, R. Gray and C. E. Clarke, Systematic review of levodopa dose equivalency reporting in Parkinson's disease, *Movement Disorders* **25** (2010) 2649–2653.
26. E. D. Farahani, T. Goossens, J. Wouters and A. van Wieringen, Spatiotemporal reconstruction of auditory steady-state responses to acoustic amplitude modulations: Potential sources beyond the auditory pathway, *NeuroImage* **148** (2017) 240–253.
27. D. D. Cummins, R. B. Kochanski, R. Gilron, N. C. Swann, S. Little, L. H. Hammer and P. A. Starr, Chronic sensing of subthalamic local field potentials: Comparison of first and second generation implantable bidirectional systems within a single subject, *Front. Neurosci.* **15** (2021) 725797.
28. G. M. Bidelman, Subcortical sources dominate the neuroelectric auditory frequency-following response to speech, *NeuroImage* **175** (2018) 56–69.
29. N. Bigdely-Shamlo, T. Mullen, C. Kothe, K.-M. Su and K. A. Robbins, The PREP pipeline: Standardized preprocessing for large-scale EEG analysis, *Front. Neuroinform.* **9** (2015) 16.
30. R. Oostenveld, P. Fries, E. Maris and J.-M. Schoffelen, FieldTrip: Open source software for advanced analysis of MEG, EEG, and invasive electrophysiological data, *Comput. Intell. Neurosci.* **2011** (2011) 1–9.
31. J. Hou, K. Morgan, D. M. Tucker, A. Konyn, C. Poulsen, Y. Tanaka, E. W. Anderson and P. Luu, An improved artifacts removal method for high dimensional EEG, *J. Neurosci. Methods* **268** (2016) 31–42.
32. T. Goossens, C. Vercammen, J. Wouters and A. van Wieringen, Aging affects neural synchronization to speech-related acoustic modulations, *Front. Aging Neurosci.* **8** (2016) 133.
33. A. Sergeeva, C. B. Christensen and P. Kidmose, Towards ASSR-based hearing assessment using natural sounds, *J. Neural Eng.* **21** (2024) 026045.
34. Y. Zhang, G. Zhou, J. Jin, X. Wang and A. Cichocki, Frequency recognition in SSVEP-based BCI using multiset canonical correlation analysis, *Int. J. Neural Syst.* **24** (2014) 1450013.
35. B. Wittevrongel and M. M. V. Hulle, Frequency- and phase encoded SSVEP using spatiotemporal beamforming, *PLoS One* **11** (2016) e0159988.
36. N. Kaongoen and S. Jo, A novel hybrid auditory BCI paradigm combining ASSR and P300, *J. Neurosci. Methods* **279** (2017) 44–51.
37. Y. Jiao, Y. Zhang, Y. Wang, B. Wang, J. Jin and X. Wang, A novel multilayer correlation maximization model for improving CCA-based frequency recognition in SSVEP brain-computer interface, *Int. J. Neural Syst.* **28** (2018) 1750039.
38. Y. Benjamini and Y. Hochberg, Controlling the false discovery rate: A practical and powerful approach to

multiple testing, *J. Roy. Stat. Soc. Ser. B: Stat. Methodol.* **57** (1995) 289–300.
39. V. Litvak, E. Florin, G. Tamás, S. Groppa and M. Muthuraman, EEG and MEG primers for tracking DBS network effects, *NeuroImage* **224** (2021) 117447.
40. A. Alhourani, M. M. McDowell, M. J. Randazzo, T. A. Wozny, E. D. Kondylis, W. J. Lipski, S. Beck, J. F. Karp, A. S. Ghuman and R. M. Richardson, Network effects of deep brain stimulation, *J. Neurophysiol.* **114** (2015) 2105–2117.
41. D. Guehl, P. Burbaud, C. Lorenzi, C. Ramos, B. Bioulac, C. Semal and L. Demany, Auditory temporal processing in Parkinson's disease, *Neuropsychol.* **46**(9) (2008) 2326–2335.
42. B. Kolomiets, J. Deniau, J. Glowinski and A. Thierry, Basal ganglia and processing of cortical information: Functional interactions between trans-striatal and trans-subthalamic circuits in the substantia nigra pars reticulata, *Neuroscience* **117** (2003) 931–938.
43. P. J. Magill, A. Sharott, M. D. Bevan, P. Brown and J. P. Bolam, Synchronous unit activity and local field potentials evoked in the subthalamic nucleus by cortical stimulation, *J. Neurophysiol.* **92** (2004) 700–714.
44. R. Tomioka, N. Shigematsu, T. Miyashita, Y. Takahashi, M. Yamamoto, Y. Yoshimura, K. Kobayashi, Y. Yanagawa, N. Tamamaki, T. Fukuda and W.-J. Song, The external globus pallidus as the hub of the auditory cortico-basal ganglia loop, *Eneuro* **11** (2024) ENEURO.0161–24.2024.
45. R. Tomioka, M. Takemoto and W.-J. Song, Anatomical pathways and functional implications of the rodent auditory system-basal ganglia interconnectivity, *Front. Behav. Neurosci.* **19** (2025) 1645035.
46. M. De Letter, A. Bruggeman, K. De Keyser, P. Van Mierlo, H. Buysse, D. Van Roost and P. Santens, Subthalamic nucleus activity in the processing of body and mental action verbs in people with Parkinson's disease, *Brain Lang.* **202** (2020) 104738.
47. T. D. Johnson, A. J. Gallagher, S. Coulson and L. M. Rangel, Network resonance and the auditory steady state response, *Sci. Rep.* **14** (2024) 16799.
48. A. Toso, A. P. Wermuth, A. Arazi, A. Braun, T. G. t Jong, P. J. Uhlhaas and T. H. Donner, 40 hz steady-state response in human auditory cortex is shaped by gabaergic neuronal inhibition, *J. Neurosci.* **44** (2024) e2029232024.

Int. J. Neur. Syst. 2025.35. Downloaded from www.worldscientific.com
by KATHOLIEKE UNIVERSITEIT LEUVEN on 12/23/25. Re-use and distribution is strictly not permitted, except for Open Access articles.